On the Reliability of Error Localization Indicators

R. Pascual, J.C. Golinval, M. Razeto
Université de Liège, LTAS, 21, rue E. Solvay (C3),4000 Liège, Belgium
http://isis.ltas.ulg.ac.be/golinval/page.html
Universidad de Concepción, Casilla 53-C, Concepción, Chile
http://www.udec.cl

Abstract

An increasingly used approach for health monitoring is based on error localization techniques. They are applied on an analytical model of the nominally healthy structure and produce local values of discrepancies between the model and the measurements. In this way, damaged regions are identified, and the selection of the model parameters (to be updated) becomes easier. This helps the optimization procedure to reconciliate the model and the measurements, since the design space is reduced. Among the different techniques used to indicate regions where the analytical model presents parameter errors, one finds those that are based on output comparison: COMAC, MAC variation. These methods quantify the loose of correlation between paired modes associated to a degree of freedom. They assume that local model errors produce local changes in the modes (which is a case dependent assumption). They present the advantage of not requiring the use of expansion or reduction techniques but they are limited by the mode pairing process and by the norms used for the comparison. Another approach is to use the model equilibrium conditions. In this category, one finds the force residual technique and the method based on the minimization of errors on constitutive equations (MECE). A drawback of these techniques is that they require a matching process *a priori*. The aim of this paper is to analyze the limitations of this last class of techniques to locate model errors.

Nomenclature

K, M	FE model matrices
K^*, v^*, ω_{v^*}, M^*, v^*, q^*	perfectly identified expanded vectors, frequency, matrices, modal displacements
$\triangle K$, $\triangle M$	errors of the model matrices
v	expanded experimental shape
ΔZ	$\Delta K - \omega_{\bar{v}}^2 \Delta M$
$\triangle v$	error in the expanded vector
$\triangle \omega$	error in the identification of the experimental eigenfrequency
f_r	residual force when v and $\omega_{\bar{v}}$ are applied, $f_r = Zv$
Z	$K - \omega_{\bar{v}}^2 M$
$\tilde{M}, \tilde{K}, \tilde{q}, \tilde{T}$	SEREP variables
$\hat{q}$	MECE modal displacements
Φ	model modal matrix
$_1$	measured partition of dofs
n	noise term
α	control parameter
u	instrument shape vector
K_s	stiffness matrix of the substructure s
Φ_1^+	pseudo inverse of Φ_1

1. Introduction

Error localization methods may be based (or not) on a numerical model. Non model based techniques assume that local model errors produce local changes in the responses. They are limited by the number of sensors and may be used by comparing modal indicator variations with regard to a previous healthy situation. Evolution of the damage influence on the response can be tracked in this way, but it cannot assess if the structure is still reliable or safe. However, they present the advantage of not requiring the expensive process of building a model. Reference [6] presents an extensive survey.

Model based damage identification methods allow to detect not only the location of changes in the structure, but also its nature, and its amplitude level. The engineer may have a better understanding of the physics behind the damage, and is able to exploit the rich knowledge base used to build the model.

In this contribution, some limitations of the model based error localization process are highlighted. In order to be self contained, first a brief explanation of the expansion techniques is presented. Then the error localization technique is explained. Four causes for poor localization results are discussed. Several numerical and experimental examples will help the reader to focus on the main ideas.

2. Theoretical Background

Let us assume that the model *structure* errors are negligible (equations are correct, discretization is adequate), but that model *parameter* errors (material properties, geometric properties) exist. Under these conditions,the equilibrium equation for an eigenmode of the experimental structure may be written as

$$K^* \; v^* = \omega_{v^*}^2 \; M^* \; v^* \tag{1}$$

The validity of the approach is crucial for the rest of the developments. The only way to assess that equation (1) holds (at least to some extent and for a limited frequency range) is by using linearity checks, verifying the quality of the model using correlation techniques like MAC, verifying that identified modal shapes are at most slightly complex quantities, etc. The assumption of such a structural model tells implicitly that the "damaged" experimental structure shows a linear behavior and that dissipative effects do not influence normal modes.

The relation with the initial FE model matrices K, M can be established through the following relations

$$K^* = K + \triangle K \tag{2}$$

$$M^* = M + \triangle M \tag{3}$$

$$v^* = v + \triangle v \tag{4}$$

$$\omega_{v^*} = \omega_{\bar{v}} + \triangle\omega \tag{5}$$

The approximation to the experimental mode, v, is found by assuming that the numerical model is close to the true structure. Using a standard formulation, it can be shown that the idea is to minimize the residues of the equilibrium equation in some adequate metric:

$$\min \, (Z \; v)^T \; \Theta \; (Z \; v) = f_r^T \; \Theta \; f_r \tag{6}$$

Hemez [2] uses the identity matrix as weight, MECE uses the static flexibility matrix [5], Alvin [4] uses the squared static flexibility matrix.

In order to solve problem (6), the experimental data is exploited by requiring that the expanded vectors should be similar to the reference measured shapes:

$$\min \, (v_1 - \bar{v})^T \; \Xi \; (v_1 - \bar{v}) \tag{7}$$

While a large list of expansion techniques constrain the equation (7) to vanish and solve just (6), here, the relaxed expansion methods will be considered: the System Equivalent Reduction Expansion Process -SEREP- expansion [1], and the MECE expansion [5].

2.1 SEREP expansion[1]

Instead of solving (6) and (7) simultaneously, only (7) will be considered. Let the vector of measured coordinates $\bar{v}$ be expressed in terms of the reduced model modal base:

$$\bar{v} \approx \Phi_1 \; q^* + n \tag{8}$$

If an approximation $\tilde{q}$ for the true vector q^* is available, the expanded vector v can be expressed as:

$$v = \Phi \; \tilde{q} \tag{9}$$

From equation (8), the modal displacements may be estimated by

$$\tilde{q} = \Phi_1^+ \; \bar{v} \tag{10}$$

Alternatively, the expanded vector can be expressed in terms of the SEREP operator:

$$\tilde{v} = \tilde{T} \; \bar{v} \tag{11}$$

where

$$\tilde{T} = \Phi \; \Phi_1^+ \tag{12}$$

The SEREP operator allows to define the reduced system matrices:

$$\begin{aligned} \tilde{M} &= \tilde{T}^T \; M \; \tilde{T} \\ \tilde{K} &= \tilde{T}^T \; K \; \tilde{T} \end{aligned} \tag{13}$$

2.2 MECE expansion [5]

If metric $\Theta = K^{-1}$ is chosen to solve problem (6) and $\Xi = \tilde{K}$ in equation (7), both equations can be considered simultaneously by solving the optimization problem

$$\min (Z\ v)^T\ \Theta\ (Z\ v) + \alpha\,(v_1 - \bar{v})^T\,\Xi\,(v_1 - \bar{v}) \tag{14}$$

The MECE expansion problem (14) may be expressed as

$$\min (v - u)\,K\,(v - u) + \alpha\,(v_1 - \bar{v})\,\tilde{K}\,(v_1 - \bar{v}) \tag{15}$$

subject to

$$K\ u = \omega_{\bar{v}}^2\ M\ v \tag{16}$$

where u is an instrument shape vector. In order to solve the problem, the expanded vector is also expressed as a combination of the numerical modal base. In equation (15) $\tilde{K}$ assures a good balance between the two terms, but other weight matrices may be used.

Equation (15) can also be written as

$$\min (v - u)^T\,K\,(v - u) + \alpha\,(\tilde{v} - v)^T\,K\,(\tilde{v} - v) \tag{17}$$

If K and M are expressed in terms of the numerical modal base, the following result is obtained

$$(\hat{q})_i = \frac{\alpha}{\left(1 - (\omega_{\bar{v}}/\omega_i)^2\right)^2 + \alpha}\,(\tilde{q})_i \tag{18}$$

For each mode, MECE not only takes into account the correlation and the relative energy between the analytical and experimental eigenmodes, as SEREP, but also the frequency shift, weighted with α. If there is no frequency shift, the frequency dependent coefficient is always 1. As can be seen for the majority of the modes, both methods will lead to almost the same modal displacements. SEREP can be regarded as a simplified MECE solution. Equation (18) provides a cheap way to get the MECE expanded vectors.

2.3 Error localization

Error localization methods seek for the locations on the structural model where discrepancies between experimental and numerical results may be present (damage, if health monitoring is the aim). The convenient introduction of the instrument vector u in equation (16) allows the definition of an error indicator that quantifies a residual strain energy (element-by-element, substructure-by-substructure):

$$e_s = (u - v)\,K_s\,(u - v) \tag{19}$$

where K_s is the stiffness matrix of the substructure s.

3. Limitations of the MECE localization

In this section, some limitations for a correct error localization using the MECE technique will be highlighted. It will be seen that even excluding the effects of noise on the measurements, several perturbing situations appear.

3.1 Energy dispersion

It is easy to show from equation (6) and (16) that the residual displacement is the solution of the equivalent static problem:

$$K\ (v - u) = f_r \tag{20}$$

To simplify the analysis, let us assume that no noise is present in the measures, and that expansion is perfect. Then the following equality holds:

$$v = v^*$$

so that

$$K\ (v - u) = \triangle Z\ v^* \tag{21}$$

Looking at this equation as a standard static problem, it appears that the excitation force vector $\triangle Z\ v^*$ is applied only on the dofs associated to the erroneously modeled substructures. The solution to problem (21) results in propagated deformations all over the structure in general. For this reason, the strain energy error indicator (19) will show residual energies all throughout the structure.

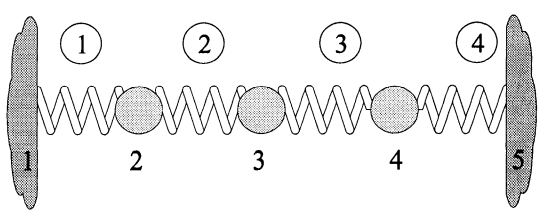

Figure 1: 3-dofs structure

This fact can be illustrated on the 3-dofs structure represented in figure 1. In this example, all springs and masses have a unitary value. The experimental structure has been simulated by stiffening the spring between dofs 1 and 2 (100% stiffness increase). Only dofs 2 to 4 are supposed to be measured. Modes have been "identified" without noise. Expansion in this case is not needed. Error localization shows normalized values as shown in figure (2). All 3 "identified" modes allow to locate the error, but a situation appears: even having no expansion errors, nor noise, residual energy is dispersed all over the structure.

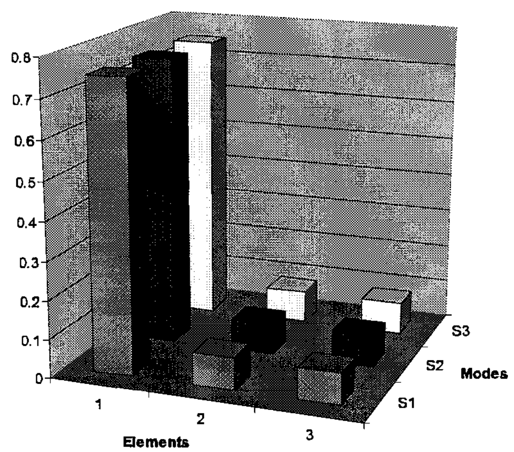

Figure 2: $\frac{(u-v)^T K_s (u-v)}{(u-v)^T K (u-v)}$

For each mode, the wrongly modeled substructure (spring between dofs 1 and 2) concentrates 75% ; of the residual energy while the other elements keep 8.33% each. This situation can be understood by condensing the system matrices to the dof where the residual force actuates. It is seen that the wrongly modeled spring carries 75% of the statically condensed stiffness, while the rest just 25%. Then, the ratio between the residual energy of the rest of the structure and the energy on spring 1 is a constant:

$$e_{rest}/e_1 = 1/3 \tag{22}$$

In the following, this ratio will be called the "attachment ratio".

In general, each substructure of a model will be "attached" in a particular way to the rest of the structure producing different values for the ratio. The ideal situation to have consistent localization would be to have a zero ratio at all dofs of each element.

3.2 Non excitation of model errors

It can be easily shown that the force residue defined in equation (6) is a sum of two terms:

$$-f_r = Z \triangle v + \triangle Z \ v^* \tag{23}$$

where the first term is dependent on the criterion used for expansion and the second one is a constant.

If errors are localized, the non spurious component of the residual force is a sparse vector, almost full of zeros. Non null values are dependent on the ability of the real vector v to deform the substructures that present errors ($\triangle Z$):

$$\triangle Z \ v^* \gg 0 \tag{24}$$

On the other hand, the effects of the spurious components of the expanded vector are easily amplified since they are weighted by the whole dynamic stiffness matrix, generating force components all over the structure.

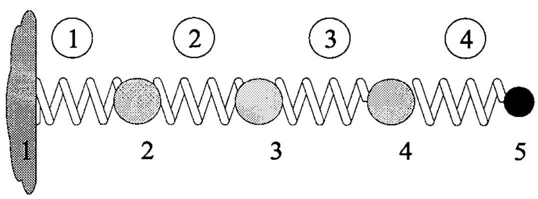

Figure 3: 4-dofs structure

A potentially dangerous situation for error localization is to identify a group of modes that do not excite the error:

$$\triangle Z \ v^* \approx 0 \tag{25}$$

In this case, $u - v$ comes only from expansion errors; so that localization becomes systematically erroneous. This mode is *blind* to model errors. The problem is that in real life, the spurious part Δv is always present at some level, so that erroneous localization results may happen.

To clarify the idea, an example very similar to the one previously described is considered. The structure initially is the same as in the first example. Here, the fixation at dof 5 has been removed and an extra mass of 0.001 has been added at the free end . (figure 3). The "experimental" structure presents the same error as before: a doubled stiffness constant on spring 1. Modes have been "identified" on dofs 2 to 5, without noise. Expansion is not needed either. The error localization shows normalized values as shown in figure 4.

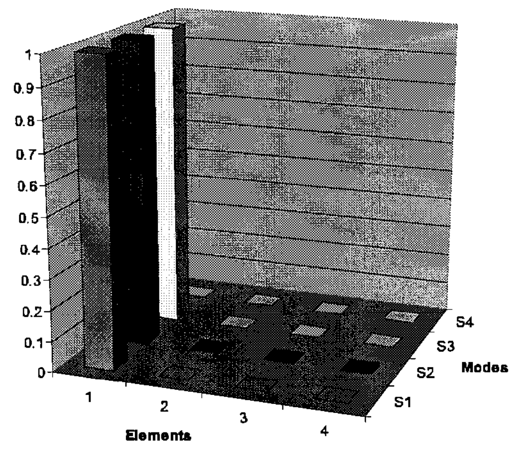

Figure 4: $\frac{(u-v)^T K_s (u-v)}{(u-v)^T K (u-v)}$

For modes 1 to 3, the indicator concentrates 100% of the residual energy on the erroneous element. This can be understood by statically condensing the structure to dof 2, where the residual force applies. The attachment ratio in this case is ideal $e_{rest}/e_1 = 0$. Mode 4 is more interesting since only the small mass at the end vibrates, exciting exclusively the spring between dofs 4 and 5 (figure 5), so that equation (25) holds. As the error does not excite the mode, the indicator is ineffective to locate the error for this particular mode.

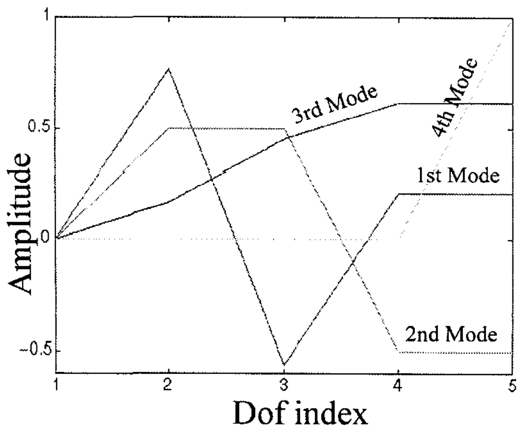

Figure 5: 4 dofs model eigenmodes

A necessary condition for a correct localization is that the physical part of the expanded vector excites the "wrong" substructure in a non *negligible* way; and in good ratio regarding to the spurious part of the expanded vector. The level for *negligible* is not clear, since the true expanded vector is not known.

By averaging the normalized residual energies for all the identified modes (a common approach), the correct error can still be found. In a general situation this would not be necessarily the case. It is common to identify only the low frequency global modes. For a robust localization, it is necessary that the error excites a majority of the modes in order to filter out the spurious error zones which are always present to some extent in the localization equation (19).

3.3 Poor expansion base

From equation (16)

$$u = K^{-1}\ \omega_{\bar{v}}^2\ M\ v \tag{26}$$

If the spectral development of K^{-1} is used, u can also be expressed as

$$u = \omega_{\bar{v}}^2 \sum_{i=1}^{N} \frac{\phi_i\ \phi_i^T}{\omega_i^2\ \mu_i}\ M\ \left(\sum_{j=1}^{NS} \hat{q}_j\ \phi_j\right)$$

which can be simplified into

$$u = \sum_{i=1}^{NS} \left(\frac{\omega_{\bar{v}}}{\omega_i}\right)^2 \hat{q}_i\ \phi_i$$

This results allows to express the content of the residual vector $v - u$, whose strain energy distribution will be used for error localization:

$$v - u = \sum_{i=1}^{NS} \left(1 - \left(\frac{\omega_{\bar{v}}}{\omega_i}\right)^2\right) \hat{q}_i\ \phi_i \tag{27}$$

Since $v - u$ is built by combining a limited set of mode shapes, its energy content will be limited to what the used modes are able to represent.

Equation (27) produces a smooth distribution of residual energy. It seems necessary to enrich the expansion base with vectors able to reproduce the residual force in a more accurate way. An analysis of the energy distribution of the expansion base allows an *a priori* estimation of localization limitations.

3.4 Inaccurate expansion

A cause of problems for an expansion using the projections into the FE modal base happens when a subset of numerical modes is badly represented in the set of measured dofs. Two situations may appear:

- two or more reduced modes are (almost) identical;
- one or more modes are (almost) not existent in the set of measured dofs.

For the first case, Φ_1 in equation (8) will present at least two vectors which are linearly dependent. The pseudo inverse in equation (10) will disperse the $(\tilde{q})_i$ values in order to minimize the distance $|\Phi_1 \tilde{q} - \bar{v}|$. SEREP will provide an erroneous projection. MECE will also suffer this situation due to the use of equation (18).

For the second case, any correlation between the measured mode and the almost not existent mode will produce a high modal displacement value in that direction, as shown in figure 6, where the mode ϕ_j is a poorly represented numerical mode shape.

Figure 6: Poor expansion base

This idea is illustrated on an experimental laboratory structure consisting of a reinforced concrete beam with dimensions $6m \times 0.2m \times 0.25m$ (figure 7). The beam was damaged by applying static loads and presents cracks along the lower face. The boundaries can be considered to be "free-free" conditions. Excitation is applied in one of the corners so that flexion and torsion modes are excited. Accelerations are measured on both sides of the top face of the beam at 62 points. 10 experimental modes are identified. A detailed explanation of the setup can be found in reference [7].

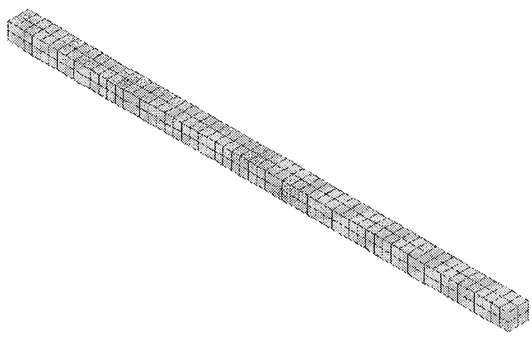

Figure 7: Beam model

A 3D FE model of the beam was developed using $60 \times 2 \times 2$ shell elements. A MECE expansion using equation (18) was performed using a modal base consisting of the first 20 modes of the model. In order to evaluate the quality of the expansion, the experimental expanded modes are compared to their FE counterparts by using the MAC as shown in figure 8. Something appears wrong in the expansion since the expanded modes are dominated by only 3 FE modes and are highly linearly dependent. The diagonal dominant pattern of the MAC matrix has been lost.

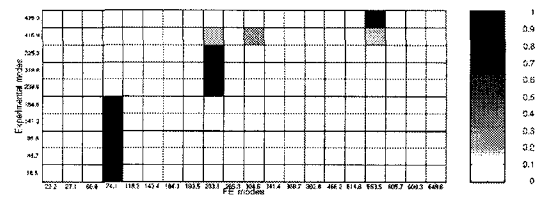

Figure 8: Erroneous expansion results

Considering the problems previously introduced, first the linear independence of the reduced numerical base is analyzed using the MAC as shown in figure 9. There, the FE reduced base is compared against herself: each mode is quite independent of the rest.

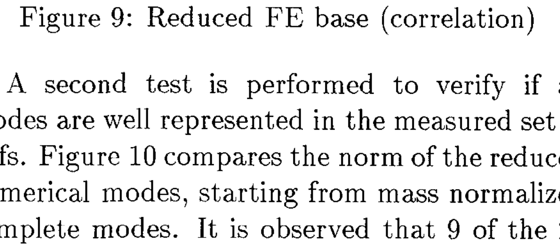

Figure 9: Reduced FE base (correlation)

A second test is performed to verify if all modes are well represented in the measured set of dofs. Figure 10 compares the norm of the reduced numerical modes, starting from mass normalized complete modes. It is observed that 9 of the 20 modes are very poorly present. This situation is expected since these modes are all perpendicular to the measurements plane (axial deformations and second plane flexion shapes).

The problem is easily solved in this case by removing all these modes from the expansion base. Now the MAC between the expanded experimental vectors and the numerical modes retrieves its diagonal dominant form (figure 11).

This example shows how the combination of a poor sensor setup and an ill conditioned ex-

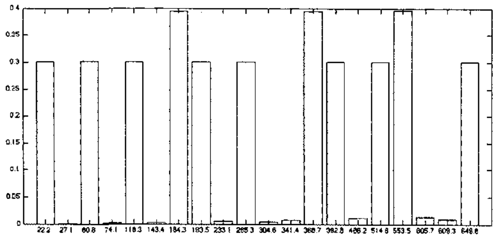

Figure 10: Reduced FE base (norm)

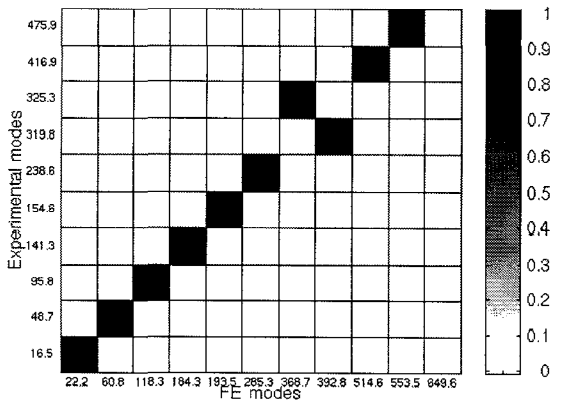

Figure 11: Improved expanded base compared to FE base

pansion base may induce severe expansion/error localization results. In the literature, there exists methods to assure an optimal configuration of a limited set of sensors in order to provide a well defined base [3].

4. Civil engineering structure example

The case has been exploited in details in the literature [6]. It is the I-40 bridge over the Rio Grande river in New Mexico. Figure 12 shows the model of the bridge subject to its first mode shape.

The real structure was tested in its undamaged state using ambient and force excitations. Damage was induced by cutting through one of the main girders in four increasing states (figures 13 and 14). Modal analysis was performed in each state using a set of 26 accelerometers placed along the two sides of the bridge deck.

According to the evolution of the frequencies and MAC values, it is observed that no significant changes appear in the eigenfrequencies and the MAC until the last state of damage (figures 15 and 16). Mode shapes which show nodal behav-

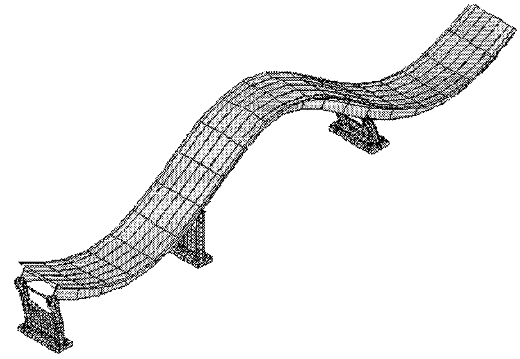

Figure 12: FE model of the bridge-1st mode

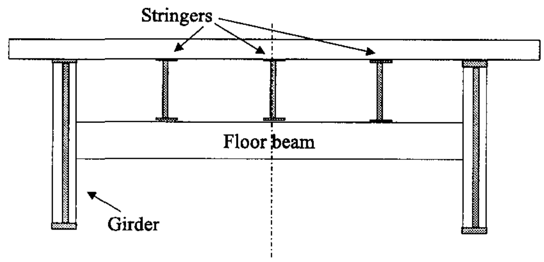

Figure 13: Bridge cross section

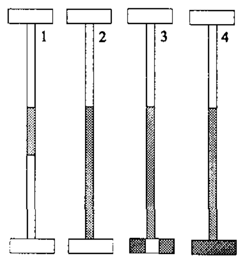

Figure 14: Section of the damaged girder

ior near the damage location are not significantly perturbed at all states (modes 3 and 5). Only modes 1 and 2 show an important change for the last state of damage.

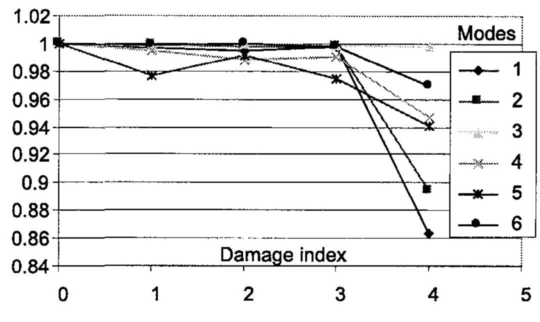

Figure 15: MAC evolution

Results of the MECE error localization are shown in figure (17) for the first mode and for

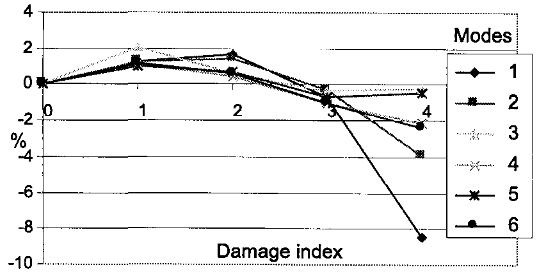

Figure 16: Frequency evolution

the last state of damage. The zone where the cut was produced is clearly indicated.

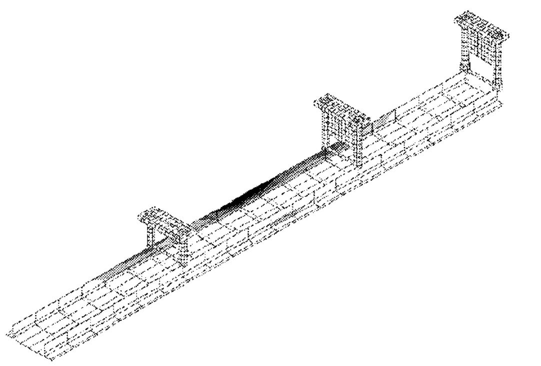

Figure 17: Error localization for the first mode

For previous states of damage, the localization is not so clear. The main girders concentrate almost all of the residual energy but it is dispersed all over their length. The evolution of the residual energy against the damage situation is summarized in figure 18. On the y-axis the maximal value of residual energy is shown. It is observed that the indicator is insensible to the first 3 damage situations.

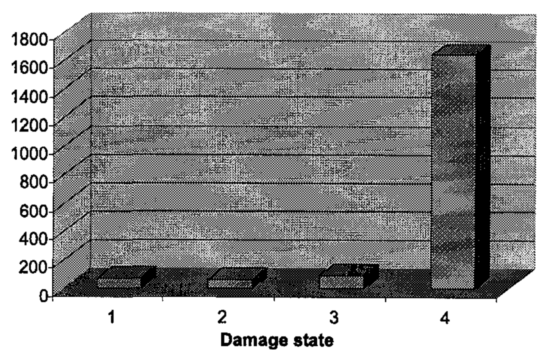

Figure 18: Evolution of the error indicator

It may be assumed that localization difficulties arise, in first place, due to the violation of equation (1). This is so, since bridges are, to some extent, time-variant systems (humidity, temperature changes, non viscous damping,..). Measurements change from test to test so that the identified modal properties are not constant. It results that difficulties described in section 4 become more important: several experimental modes shapes are quite insensitive to the development of the damage in the measured dofs (section 3.2). The sensor configuration and the limited size of the expansion modal base also limit the quality of the localization (section 3.3). The noisy environment and the modal analysis technique may induce an unstable estimation of the expansion coefficients (section 3.4). Of course the energy dispersion problem (section 3.1) appears also, but this is an implicit phenomenon of the localization technique.

Compared to other localization approaches already used [6], the MECE results show the same sensitivity to the damage state. But, since a model has been used, it is clear that a dominant stiffness error has appeared on the girder. Model updating would lead to an improved model of the bridge. From a correlated model, it is possible to establish if the bridge is still reliable, and/or the modifications that it needs to attain a given level of security. This is not the case for the non model based techniques.

5. Final remarks

Several problems related to the use of model based error localization techniques have been highlighted. Topics like model structure validity, error localization dispersion, model error excitation, richness of the expansion modal base and reliability of the expansion due to noise and sensor setup have been examined and illustrated through several numerical and experimental examples.

In the near future, topics like the direct application of forced responses, the optimization of the sensor setup to assure a reliable expansion, the enrichment of the expansion modal base for improved localization results and the development of an *a priori* indicator of localization limitations are foreseen.

Acknowledgements

Part of this text presents research results of the Belgian programme on Inter-university Poles of attraction initiated by the Belgian state, Prime Minister's Office, Science Policy Programming. The scientific responsibility is assumed by its authors.

The authors want to thank Prof. G. De Roeck and Dr. B. Peeters from the Katholieke Universiteit Leuven (Belgium) for providing all the necessary data regarding to beam test case.

They also want to thank Dr. S. Doebling from Los Alamos National Laboratory (USA) for providing the measurement data and the FE model that lead to the results obtained in the case of the I-40 bridge.

References

1. OCallahan J., Avitabile, P., *System Equivalent Reduction Expansion Process (SEREP)*, Proceedings of the 7th International Modal Analysis Conference, Las Vegas, Nevada, pp 29-37,(1989).
2. Hemez, F., *Theoretical and experimental correlation between finite elements models and modal tests in the context of large flexible space structures*, Ph.D. dissertation, Univ. of Colorado, (1993).
3. Kammer, D.C., Yao, L., *Enhancement of on-orbit modal identification of large space structures through sensor placement*, Journal of Sound and Vibration, 171(1), pp. 119-139, (1994).
4. Alvin, K.F., *Finite element model update via bayesian estimation and minimization of dynamic residuals*, XIV Intl. Modal Anal. Conf., Orlando, Dearborn, Michigan, pp. 561-567, (1996).
5. Collignon, P., Golinval, J.C., *Comparison of model updating methods adapted to local error detection*, Intl. Conf. on Noise & Vib. Eng.,21th ISMA, Leuven, Belgium, (1996).
6. Doebling, S. W., Farrar, C.R., Prime, M.B., Shevitz, D.W., *Damage Identification and Health Monitoring of Structural and Mechanical Systems from Changes in Their Vibration Characteristics: A Literature Review*, Los Alamos National Laboratory Report LA-13070-MS, (1996).
7. Maeck, J., Abdel Wahab, M., De Roeck, G., *Damage detection in reinforced concrete structures by dynamic system identification*, ISMA23, Leuven, Belgium, (1998).